Title: Systemic Calcitonin Gene-Related Peptide (CGRP) modifies auditory and vestibular endorgan electrical potentials, and increases auditory and vestibular hypersensitivities: Implications for vestibular migraine

Abbreviated Title: CGRP's effect on inner ear endorgan and behavior

Authors: Shafaqat M. Rahman[1], Benjamin Liang[1], Stefanie Faucher[1], Elana Fine[1], Raajan Jonnala[1], Joseph C. Holt[2,3], Choongheon Lee[3], Anne E. Luebke[1,2*]

Affiliations:

[1]University of Rochester, Department of Biomedical Engineering, Rochester, NY 14627

[2]University of Rochester Medical Center, Department of Neuroscience, Del Monte Institute of Neuroscience, Rochester, NY 14642

[3]University of Rochester Medical Center, Department of Otolaryngology, Rochester, NY 14642

*Corresponding author: Anne E. Luebke, aluebke@ur.rochester.edu

Number of Pages: 21

Number of Figures: 3

Number of Tables: 0

Number of words for Abstract: 238

Number of words for Significance Statement: 116

Number of words for Introduction: 344

Number of words for Discussion: 618

Conflict of interest statement: The authors declare no competing financial interests.

Acknowledgments: This work was fully supported by NIH R01DC017261.

Abstract:

Migraine is a severe and chronic neurological disorder that affects ~18% of people worldwide, the majority being female (3:1). It is characterized by recurrent, debilitating headaches and heightened sensory sensitivities. People with migraine may also experience a heightened motion sensitivity that leads to episodes of vertigo and imbalance, termed vestibular migraine (VM). Calcitonin Gene-Related Peptide (CGRP) is implicated in migraine and is believed to act on brain meninges, midbrain, brainstem, or directly on ganglia. CGRP-based antagonists have shown efficacy for migraine treatment. CGRP also signals at efferent synapses of the cochlea and vestibular endorgans, but it is unclear if exogenous CGRP can modulate inner ear function at the endorgan, and cause heightened behavioral responses consistent with VM. We tested if intraperitoneally (IP) delivered CGRP to wildtype mice can modulate endorgan potentials to sound [via auditory brainstem responses (ABRs)] and jerk stimuli [via vestibular sensory evoked potentials (VsEPs)]. We also assessed behavioral measures of phonophobia [acoustic startle reflex (ASR)] and static imbalance [postural sway-center of pressure (CoP)] after IP CGRP, and observed female mice exhibited heightened sensitivities to IP CGRP in all assays. Male mice showed similar auditory sensitivity and endorgan effects to CGRP but systemic CGRP did not modify male postural sway as it did in females. In conclusion, we show that systemically delivered CGRP modulates activity of the auditory and vestibular endorgan responses, and elicits behavioral effects that are consistent with symptoms in a disorder like VM.

Significance statement:

Calcitonin Gene-Related Peptide (CGRP) has been implicated in migraine, and CGRP-based therapeutics have shown efficacy in the treatment of migraine headaches. CGRP is also present in efferent synapses of the inner ear, so we questioned if increases in systemic CGRP can act directly on inner ear endorgans and modify corresponding behavioral responses. In this study, we determined systemic CGRP changes cochlear and vestibular endorgan potentials and produces migraine behaviors similar to phonophobia and postural control deficits. Peripheral changes in auditory and vestibular compound action potentials following systemic CGRP administration suggest CGRP can act directly on

50 the inner ear, which provides a one site of action for CGRP's involvement in hypersensitivity to sound
51 and movement in migraine.
52
53 **Introduction:**
54 Migraine is a debilitating chronic neurological disorder that is listed by the World Health Organization
55 (WHO) as the most debilitating neurological disorder worldwide and is estimated to affect 18% of
56 women and 6% of men (Goadsby, Lipton, and Ferrari 2002; Lipton et al. 2007). About 42% of people
57 with migraine have a vestibular component causing balance problems and dizziness (Kuritzky, Toglia,
58 and Thomas 1981; Neuhauser et al. 2001; Neuhauser 2007, 2009), termed vestibular migraine (VM).
59 VM is a major cause of vertigo in dizziness clinics (Kayan and Hood 1984) and patients with migraine,
60 and especially VM, exhibit a heightened sense of sound and motion (Ashkenazi et al. 2009; Lopez-
61 Escamez et al. 2014). Despite migraine and VM's prevalence, the pathophysiology remains uncertain
62 (Lempert et al. 2022; Lempert et al. 2012).
63
64 Calcitonin gene-related peptide (CGRP) is intensively studied for its role in migraine's sensory
65 hypersensitivities (Russo 2015). CGRP levels are elevated during migraine, and normalization of
66 CGRP levels is associated with the relief of headache pain which is thought to act at either brain
67 meninges or the trigeminal system (Goadsby, Lipton, and Ferrari 2002; Juhasz et al. 2005; Lassen et
68 al. 2002). CGRP also signals at efferent synapses of the cochlea and vestibular endorgans, so we
69 questioned if elevated CGRP levels in migraine could directly affect the inner ear. To that end, we
70 modeled the increase in CGRP during migraine by a systemic intraperitoneal (IP) injection to determine
71 if systemic CGRP can modulate activity of these endorgans (Dickerson et al. 2016; Luebke et al. 2014;
72 Maison et al. 2003). We also questioned if increases in systemic CGRP can cause behaviors
73 suggestive of heightened auditory and vestibular sway consistent with VM.
74
75 In this study, we tested wildtype C57BL/6 mice to determine if there is a change in endorgan potentials
76 to sound (measured using auditory brainstem responses - ABRs) and jerk stimulus (measured using
77 vestibular stimulus evoked potentials - VsEPs) after a CGRP injection. We also assessed

corresponding behavioral measures of phonophobia (acoustic startle reflex – ASR) and imbalance (postural sway/center of pressure - CoP) after systemic CGRP injection.

Methods:

Animals: C57BL6/J mice were obtained from Jackson Laboratories (JAX #664) and were housed under a 12-hour day/night cycle under the care of the University Committee on Animal Resources (UCAR) at the University of Rochester. Mice were housed together in cages (5 mice per cage) with *ad libitum* access to food, water, and bedding material. A total of 74 mice (37F/ 37M) were used for these studies, which were powered sufficiently to detect male/female differences. Before experimentation, mice were equilibrated in the testing room controlled for an ambient temperature between 22-23°C for at least 30 minutes, and remained in this room until completion of experiments. Injections occurred after the equilibration period. Mice used during behavioral experiments were returned to the vivarium, while mice used for ABR/VsEP experiments were euthanized after testing. Mice tested were between 2.3 - 6 months of age. This age range in mice correlates to 20-30 years in humans, which is within the age range that patients develop migraine symptoms (Lessem 2018). All animal procedures were approved by the University of Rochester's IACUC committee and performed in accordance with NIH standards.

VsEP and ABR Protocol: C57BL/6 mice were anesthetized with IP urethane/xylazine (1.2 g/kg/20 mg/kg). VsEP and ABR recording methods have been described in detail elsewhere (Lee, Holt, and Jones 2017). Briefly, to record VsEP and ABR, subcutaneous electrodes were placed on the midline over the nuchal crest (G1), behind the right pinna (G2), and on the hip (ground). A noninvasive head clip was used to secure the mouse's head to an electromechanical shaker. During VsEPs, the shaker delivered a transient (jerk) head translation in the naso-occipital axis (± X). To confirm the absence of auditory responses during VsEP testing, a binaural forward masker (intensity: 92 dB SPL; bandwidth: 50~50 kHz) was presented with the use of a free-field speaker (FF1, TDT). For ABR recordings, the same electrodes were used to record ABRs, which were evoked by a single rectangular voltage pulse of 0.03 ms duration (corresponding to 33 kHz cut-off frequency). These click stimuli were presented via a free-field speaker, which was the same driver for acoustic masking during the VsEP recording. A

106 noninvasive rectal thermometer or thermistor was used to monitor the animals' core temperature at
107 38.0 ± 0.2°C. The standard signal averaging technique described in previous studies (Lee, Holt, and
108 Jones 2017) was used to record both VsEP and ABR, as shown in **Fig. 1A**. Recordings of both VsEP
109 and ABR were made in a soundproof booth. Both VsEPs at maximal intensity +6 dB re: 1 g/ms and
110 ABRs at maximal intensity 100 dB SPL, were recorded as a stable baseline before a single IP injection
111 of either vehicle control (PBS) or 0.1 mg/kg CGRP was given. Control amplitude and latencies are
112 depicted as the averages of the 2-3 measurements taken during baseline before injection. Following
113 single IP injection of either vehicle or CGRP, VsEP and ABR recordings were continuously measured
114 where significant shifts in VsEP and ABR responses were first observed in 10 mins and reaching a
115 plateau within 15 mins of drug injection (post-CGRP; data not shown). Thus, amplitudes and latencies
116 depicted as post-saline/post-CGRP are averages of the 2-3 measurements taken after 20-30 min post-
117 injections.
118
119 <u>Drug administration</u>: Injections were performed intraperitoneally (IP) with a fine gauge (30ga) insulin
120 syringe. Dulbecco PBS served as the vehicle control. IP CGRP was prepared at 0.1 mg/kg (rat α-
121 CGRP, Sigma). Injection volumes were calibrated so that each animal received 1 injection per testing
122 day at ~100 ul. For behavioral experiments, mice were tested ~20 minutes after IP delivery of either
123 vehicle or CGRP.
124
125 <u>Behavioral test of phonophobia: Acoustic startle reflex (ASR)</u>
126 We used the acoustic startle response (ASR) to assess heightened sound sensitivity as a mouse
127 surrogate behavior for phonophobia. Experiments were conducted within a sound-attenuating room
128 (IAC, Bronx, NY) with Sonex foam lined walls. Mice were placed individually in a wire-mesh cage that
129 is 5 cm wide, 7 cm long, and 4 cm high, and having free sound penetration. The testing cage was
130 oriented so that the mouse's head faced a Tucker Davis ES2 electrostatic speaker (Masker Speaker)
131 located 46 cm directly in front of the mouse's head (60dB BBN). The startle speaker was a Radio
132 Shack tweeter that was suspended 15 cm above the mouse (80-130 dB). The acoustic startle speaker
133 and its supports, the pedestal, acrylic shelf, and the table on which the apparatus was placed were all

134 covered with echo absorbing foam and carpeting. Force of the acoustic startle response (ASR) was
135 transduced by an accelerometer and amplitude scored as integrated root mean square voltage for 100
136 ms after delivery of the ASR. Experimental stimuli were controlled, and responses were recorded
137 using custom MATLAB (MathWorks) software. We tested acoustic startle series in quiet and in noise.
138 There were 12 conditions in this session, with startle stimuli ranging from 80 to 130 dB SPL, and
139 delivered either in silence or in a continuous background noise. When present, background noise was
140 on for the duration of the inter-trial interval and broadcasted from the masker speaker, as shown
141 schematically in **Fig. 2**.
142
143 Behavioral test of postural sway
144 Postural sway was examined using the center of pressure (CoP) test which acts as a mouse surrogate
145 behavior for static imbalance. Mice were weighed and placed on a force plate designed to measure
146 forces in the X, Y, Z and moments in the XY, YZ, and XZ directions. We used the AMTI Biomechanics
147 Force platform (model HEX6x6) and AMTI automated acquisition software to obtain forces and
148 moments and then MATLAB code was used to calculate CoP measures based on a confidence ellipse
149 enclosing 95% of the CoP trajectory values recorded in a single trial. During a given test, mice were
150 first allowed to freely maneuver on the force plate for 2-5 minutes to acclimate to the novel
151 environment. An accessory plexiglass guard was placed around the force plate to prevent mice from
152 moving off the test plate. After acclimation, ~ 10 baseline trials were taken of mice with each trial
153 indicating a CoP area (resolution per CoP measurement: 300 samples per second). These trials were
154 taken when the mouse showed no movement and its four paws were touching the force platform. To
155 assess the effect of a vestibular challenge (VC), mice were then subjected to a constant orbital rotation,
156 125 rpm for 5 minutes, and were placed back onto the force platform. After a five-minute recovery
157 period, an additional 10 trials were recorded of the mouse's sway to determine post-VC effects on CoP
158 as schematized in **Fig. 3**. Mice were first tested after systemic delivery of IP vehicle (20 min after
159 injection), with sway measured before and after the VC. Four days after vehicle testing, the same mice
160 were injected with IP CGRP and were tested again 20 minutes after injection (timing correlated with
161 endorgan potential changes). While systemic CGRP's effect is believed to dissipate two to three hours

post–injection, we retested after four days to eliminate any residual dizziness due to VC or lingering CGRP effects. We staggered sequence of IP injections in some animals by injecting CGRP followed by vehicle testing on the next day. We also injected vehicle 2x to assess test/retest reliability and saw no differences. Unreasonably large CoP values (> 15 cm^2) suggested mice were either moving during the trial or that they were at the edge of the force plate, and those values were excluded based on a 10% ROUT analysis (GraphPad Prism 9.0). Even with values excluded, a minimum of eight different 95% ellipses were computed per mouse in a given testing condition. Furthermore, we excluded mice that were outliers by running a second 10% ROUT on averaged CoPs per testing condition.

Statistical Analyses

All statistical analyses were conducted in GraphPad Prism 9.5. Analyses were conducted separately in females and males. Repeated measure ANOVA (RM-ANOVA) and paired t-tests were the primary statistical tools. Tukey post hoc analysis was used to assess treatment differences in females or males, and Bonferroni post hoc analysis was used to assess treatment differences between sexes. Significance was set at $p < 0.05$ for all analyses.

Results:

IP CGRP's Effects on ABR:

Representative traces are shown for ABR recordings in female and male C57BL6/J mice **(Fig. 1B-1C)**. Female control ABR amplitudes ($n = 6$) were computed to be 3.60 ± 0.22 μV but were increased to 4.28 ± 0.25 μV after IP CGRP (one-tailed paired t-test; $t, df = 3.99, 5$; $p = 0.005$). Likewise, a similar trend was observed in males as their control amplitudes ($n = 7$) were computed to be 4.31 ± 0.5 μV and increased to 4.66 ± 0.44 μV after IP CGRP (one-tailed paired t-test; $t, df = 1.94, 6$; $p = 0.05$) **(Fig. 1F)**. Wave 1 ABR amplitudes were normalized so that post-CGRP measurements highlight the change in amplitude from their respective control measurements (Δ wave1 amplitude) **(Fig. 1G)**. When sexes are pooled ($n = 13$), a significant Δ increase of 0.50 ± 0.13 μV was observed in wave 1 amplitudes due to IP CGRP (one-tailed paired t-test**;** $t, df = 3.9,12$**;** p = 0.001). Wave 2-1 ABR latencies were calculated as the difference between P2 and P1 latencies for control and post-CGRP; however, no differences

190 were observed in latency differences **(Fig. 1H).** A separate group of mice was tested for the effects of
191 PBS as the vehicle (data not shown, *n* = 4), but no differences were seen in Δ wave1 amplitude or
192 latency differences between control and post-vehicle (Δ wave1 amplitude $_{\text{vehicle – control}}$ = -0.19 ± 0.21 μV).
193
194 <u>IP CGRP's Effects on VsEPs:</u>
195 Similar to ABR tests, representative traces are shown for VsEP recordings in females and males (**Fig.**
196 **1D-1E).** Female P1-N1 VsEP control amplitudes (*n* = 6) were computed to be 0.68 ± 0.06 μV and were
197 reduced to 0.55 ± 0.06 μV after IP CGRP (one-tailed paired t-test; *t, df* = 1.96, 5; *t* (*p* = 0.054)) **(Fig. 1I)**.
198 Likewise, male P1-N1 VsEP control amplitudes (*n* = 8) were computed to be 0.95 ± 0.10 μV but were
199 reduced significantly to 0.76 ± 0.10 μV after IP CGRP (one-tailed paired t-test; *t, df* = 3.00, 7; *p* < 0.01).
200 P1-N1 amplitudes were normalized so that post-CGRP measurements highlight the change in
201 amplitude from their respective control (Δ P1-N1 amplitude), and both sexes were additionally pooled
202 (**Fig. 1J**). When pooling all animals (*n* = 14), a significant Δ reduction of -0.16 ± 0.04 uV in P1-N1
203 amplitude is observed due to IP CGRP (one-tailed paired t-test**;** *t, df* = 3.65, 13**;** *p* = 0.002).
204
205 P1, N1, and P2 latencies were also assessed for VsEPs, and these latencies are depicted as mean ±
206 SEM for females and males during control and post-CGRP tests **(Fig. 1K).** While no significant
207 differences were observed due to IP CGRP, modest delays in P1 were observed due to IP CGRP in
208 either sex. IP CGRP increased female P1 by 26.6 microseconds and male P1 by 22.5 microseconds
209 compared to P1 control latencies. IP CGRP also increased female N1 by 30 microseconds but had no
210 effect on Male N1. However, these latency changes were not statistically significant. Comparatively in
211 mice treated with IP vehicle, no significant P1-N1 amplitude or latency differences were observed
212 between control and post-vehicle VsEP (Δ P1-N1 amplitude $_{\text{vehicle – control}}$ = -0.03 ± 0.08 μV).
213
214 <u>CGRP's effect on sound sensitivity</u>
215 Our sound sensitivity measure in the mouse model makes use of the acoustic startle response (ASR) in
216 quiet and in background noise. Mice were assessed for the effects of IP CGRP as compared to IP
217 vehicle on their baseline. The ASR experimental setup is illustrated in **Fig. 2 A** (quiet) and **Fig. 2D**

218 (background noise 60 dB). In both IP vehicle and IP CGRP injected animals, an increase in ASR was
219 detected with increasing loudness of the startle stimulus (ES). All animals tested exhibited robust
220 startle responses (*n* = 6F/ 6M). When ASR was tested after IP CGRP injection and compared to IP
221 vehicle, all animals exhibited reduced ASR thresholds in both quiet and noise. IP CGRP significantly
222 increased sound sensitivity to the startle stimulus in quiet (**Fig. 2 B, C**) and in background noise (**Fig. 2**
223 **E, F**) in both female and male mice at all sound levels ($p < 0.0001$ quiet, $p < 0.001$ in noise).
224
225 CGRP's and VC's effects on Postural Sway
226 Mice were assessed for postural sway by determining center of pressure (CoP) ellipse area. An
227 experimental timeline is shown in **Fig. 3A**. Twenty minutes after delivery of IP vehicle and without a
228 vestibular challenge (VC), group averages of 95% ellipse areas were computed to be 0.5 ± 0.06 cm^2 for
229 females and 0.4 ± 0.04 cm^2 for males **(Fig. 3B and C).** For comparison, a deadweight (toy mouse) was
230 also measured on the force platform, and its average 95% ellipse area was computed to be 0.02 ±
231 0.0005 cm^2 **(Fig. 3D).** A different cohort of mice (*n* = 10F/ 10M) was assessed for a test-retest of 95%
232 ellipse areas after IP vehicle treatment, and testing occurred four days apart. A 2-way repeated
233 measures ANOVA with Bonferroni post-hoc analysis indicated no significant differences in either sex
234 during the test-retest for females (mean difference = 0.10 ± 0.3 cm^2) or for males (mean difference = -
235 0.14 + 0.3 cm^2) ($p > 0.99$ for either sex). In either sex, 2-way ANOVAs with Tukey post hoc analyses
236 were used to assess the factors of CGRP and VC on 95% CoP ellipse areas in mice (n = 14F/ 10M)
237 **(Fig. 3E).** Differences were seen in females due to IP CGRP (F (1.00, 13.00) = 4.77, $p = 0.05$) and the
238 VC (F (1.00, 13.00) = 4.49, $p = 0.05$). In females after IP vehicle, the VC induced higher CoP ellipse
239 compared to pre-VC trials ($p = 0.02$) as shown in **Fig. 3F**. When comparing pre-VC trials, IP CGRP
240 induced increases in female CoP areas by 0.94 ± 0.23 cm^2 compared to IP vehicle ($p = 0.003$) as seen
241 in **Fig. 3G.** Females also had 0.96 ± 0.15 cm^2 higher CoP areas than males based on a separate 2-way
242 ANOVA assessing sex differences in pre-VC, CGRP and post-VC, CGRP results ($p = 0.001$).
243 The major and minor axes of 95% ellipse areas were also analyzed with 2-way ANOVAs across
244 the factors CGRP and VC (**Fig. 3H and I**). The major and minor axes lengths serve as correlates for
245 anteroposterior (AP) and mediolateral (ML) sway magnitudes. A 2-way RM ANOVA on major axes

246 indicated significant effects in females due to IP CGRP (F (1.00, 13.00) = 5.59; p = 0.03) and VC (F
247 (1.00, 13.00) = 5.41; p = 0.04) whereas these effects were not observed in males. In comparison,
248 ANOVAs that analyzed minor axes indicated a VC effect in only females (F (1.00, 13.00) = 7.46; p =
249 0.02). Tukey post-hoc indicated IP CGRP induced larger AP ellipse lengths by 0.49 + 0.10 cm in
250 females compared to their IP vehicle trials (p = 0.001). Also, in IP vehicle-treated females, there was an
251 increase in AP ellipse lengths during the post-VC test versus pre-VC (p = 0.02). IP CGRP-treated
252 females exhibited greater AP lengths compared to males during pre-VC testing by 0.57 + 0.08 cm (p <
253 0.001). ML lengths increased after the VC in IP vehicle-treated females (p = 0.02), and IP CGRP-
254 treated females had higher ML ellipse lengths compared to their IP vehicle response (p = 0.007). No
255 other significant changes were observed in AP and ML sway.
256
257 **Discussion:**
258 Using electrophysiological techniques (ABR/VsEP), we observed that intraperitoneally delivered
259 CGRP modulates endorgan function in the inner ear with a maximum 20-to-30-minutes after injection.
260 Exogenous CGRP increases wave 1 amplitudes of the ABR but reduces VsEP P1-N1 amplitudes,
261 suggesting at least one action of systemic CGRP is at the efferent signaling sites of the auditory and
262 vestibular periphery. We did not characterize wave 2 and later peaks, as we were primarily interested in
263 wave 1/P1-N1 as an indicator of sensory processing changes at the periphery.
264 Furthermore, we observed that systemic CGRP - during this 20-to-30-minute timeframe -
265 increased sound sensitivity in male and female C57BL/6J mice, whereas it only increased postural
266 sway in females.
267 A few studies in animal models have provided additional evidence for CGRP's role in vestibular
268 dysfunction and sound sensitivity. Consistent with current VsEP results where we observed delays in
269 VsEP latencies due to systemic CGRP (though not statistically significant), the loss of αCGRP
270 significantly enhanced activation timing of the macular sensors through changes at the endorgan level
271 (Jones et al. 2018). Intracerebral-ventricular (ICV) injection of nitroglycerin (NTG) caused impaired
272 balance beam walking in rats, and immunohistochemistry detected more CGRP expression in the
273 vestibular nucleus of the NTG rat model than was observed in controls. The administration of a

274 CGRP-receptor antagonist (olcegepant-BIBN4096BS) was shown to be effective in alleviating
275 impaired balance beam walking (Zhang et al. 2020; Tian et al. 2022). In addition, a recent study
276 suggested CGRP has an excitatory role in the auditory nerve response, as intra-cochlear CGRP
277 infusion was shown to enhance spontaneous and sound-driven auditory nerve activity in guinea pigs,
278 in comparison to αCGRP-null mice where a loss of nerve activity excitation was observed (Le Prell et
279 al. 2021; Allen and Luebke 2017). Thus, the auditory nerve may be hyper-sensitized to CGRP's effects
280 during a migraine.

281 Peripheral effects of systemic CGRP administration on VsEP responses is somewhat surprising,
282 as post-CGRP injection VsEP potentials were reduced and this result requires further examination in
283 future studies. However, this observation is relevant to VM, which is characterized by sensory
284 misintegration to stimuli, and thus reduced vestibular sensitivity that occurs concurrently with a
285 heightened auditory sensitivity may provide a basis for the occurrence of these symptoms.

286 Additionally, it is unclear why we did not find significant changes in males during postural sway
287 testing. While more males exhibited significant changes in their VsEP measures, we presume the lack
288 of CGRP-induced behavioral effects on sway may be due to other postural compensatory mechanisms
289 present in male mice. Yet, we did discover a robust sex difference when assessing mouse postural
290 sway, as female mice were much more affected than their male counterparts to injected CGRP.
291 Similar female-specific sexual dimorphism has been observed in other animal assays assessing
292 CGRP's effects in migraine but we are the first to show such differences in a preclinical postural sway
293 assay (Recober et al. 2009; Paige et al. 2022).

294 Small molecule blockers of the CGRP receptor ‘gepants’ have been shown to enter the
295 periphery, brainstem, and midbrain areas. Ongoing studies will determine if blocking CGRP receptor
296 signaling by small molecules (‘gepants”) or by larger monoclonal blocking antibodies (mAbs) - that may
297 or may not cross blood brain barrier (BBB), but are considered permeable to various peripheral ganglia
298 - can reduce these sound and imbalance sensitivities due to CGRP (Noseda et al. 2020; Tian et al.
299 2022; Zhang et al. 2020). The current evidence in favor of anti-CGRP mAbs for treating VM is
300 compelling, as a prospective observational cohort study over 18 months observed significant reduction

301 in vertigo and headache frequency in 50 VM patients treated with various anti-CGRP mAbs (Russo et

302 al. 2023), suggesting our preclinical findings may be dir4ectly translated to migraine patients.

303

References:

Allen, Paul D., and Anne E. Luebke. 2017. 'Reflex Modification Audiometry Reveals Dual Roles for Olivocochlear Neurotransmission', *Frontiers in Cellular Neuroscience*, 11.

Ashkenazi, A., A. Mushtaq, I. Yang, and M. L. Oshinsky. 2009. 'Ictal and interictal phonophobia in migraine-a quantitative controlled study', *Cephalalgia*, 29: 1042-8.

Dickerson, I. M., R. Bussey-Gaborski, J. C. Holt, P. M. Jordan, and A. E. Luebke. 2016. 'Maturation of suprathreshold auditory nerve activity involves cochlear CGRP-receptor complex formation', *Physiol Rep*, 4.

Goadsby, P. J., R. B. Lipton, and M. D. Ferrari. 2002. 'Migraine--current understanding and treatment', *N Engl J Med*, 346: 257-70.

Jones, S. M., S. Vijayakumar, S. A. Dow, J. C. Holt, P. M. Jordan, and A. E. Luebke. 2018. 'Loss of alpha-Calcitonin Gene-Related Peptide (alphaCGRP) Reduces Otolith Activation Timing Dynamics and Impairs Balance', *Front Mol Neurosci*, 11: 289.

Juhasz, G., T. Zsombok, B. Jakab, J. Nemeth, J. Szolcsanyi, and G. Bagdy. 2005. 'Sumatriptan causes parallel decrease in plasma calcitonin gene-related peptide (CGRP) concentration and migraine headache during nitroglycerin induced migraine attack', *Cephalalgia*, 25: 179-83.

Kayan, A., and J. D. Hood. 1984. 'Neuro-otological manifestations of migraine', *Brain*, 107 (Pt 4): 1123-42.

Kuritzky, A., U. J. Toglia, and D. Thomas. 1981. 'Vestibular function in migraine', *Headache*, 21: 110-2.

Lassen, L. H., P. A. Haderslev, V. B. Jacobsen, H. K. Iversen, B. Sperling, and J. Olesen. 2002. 'CGRP may play a causative role in migraine', *Cephalalgia*, 22: 54-61.

327 Le Prell, Colleen G., Larry F. Hughes, David F. Dolan, and Sanford C. Bledsoe. 2021. 'Effects of
328 Calcitonin-Gene-Related-Peptide on Auditory Nerve Activity', *Frontiers in Cell and*
329 *Developmental Biology*, 9.

330 Lee, C., J. C. Holt, and T. A. Jones. 2017. 'Effect of M-current modulation on mammalian vestibular
331 responses to transient head motion', *J Neurophysiol*, 118: 2991-3006.

332 Lempert, T., J. Olesen, J. Furman, J. Waterston, B. Seemungal, J. Carey, A. Bisdorff, M. Versino, S.
333 Evers, A. Kheradmand, and D. Newman-Toker. 2022. 'Vestibular migraine: Diagnostic criteria1',
334 *J Vestib Res*, 32: 1-6.

335 Lempert, T., J. Olesen, J. Furman, J. Waterston, B. Seemungal, J. Carey, A. Bisdorff, M. Versino, S.
336 Evers, and D. Newman-Toker. 2012. 'Vestibular migraine: diagnostic criteria', *J Vestib Res*, 22:
337 167-72.

338 Lessem, Sarah E. 2018. "QuickStats: Percentage of Adults Who Had a Severe Headache or Migraine
339 in the Past 3 months, by Sex and Age Grou - National Health Interview Survey, United States,
340 2018." In *Morbidity and Mortality Weekly Report (MMWR)*, edited by National Center for Health
341 Statistics.

342 Lipton, R. B., M. E. Bigal, M. Diamond, F. Freitag, M. L. Reed, W. F. Stewart, and Ampp Advisory
343 Group. 2007. 'Migraine prevalence, disease burden, and the need for preventive therapy',
344 *Neurology*, 68: 343-9.

345 Lopez-Escamez, J. A., J. Dlugaiczyk, J. Jacobs, T. Lempert, R. Teggi, M. von Brevern, and A. Bisdorff.
346 2014. 'Accompanying Symptoms Overlap during Attacks in Meniere's Disease and Vestibular
347 Migraine', *Front Neurol*, 5: 265.

348 Luebke, A. E., J. C. Holt, P. M. Jordan, Y. S. Wong, J. S. Caldwell, and K. E. Cullen. 2014. 'Loss of
349 alpha-calcitonin gene-related peptide (alphaCGRP) reduces the efficacy of the Vestibulo-ocular
350 Reflex (VOR)', *J Neurosci*, 34: 10453-8.

Maison, S. F., R. B. Emeson, J. C. Adams, A. E. Luebke, and M. C. Liberman. 2003. 'Loss of alpha CGRP reduces sound-evoked activity in the cochlear nerve', *J Neurophysiol*, 90: 2941-9.

Neuhauser, H. K. 2007. 'Epidemiology of vertigo', *Curr Opin Neurol*, 20: 40-6.

———. 2009. '[Epidemiology of dizziness and vertigo]', *Nervenarzt*, 80: 887-94.

Neuhauser, H., M. Leopold, M. von Brevern, G. Arnold, and T. Lempert. 2001. 'The interrelations of migraine, vertigo, and migrainous vertigo', *Neurology*, 56: 436-41.

Noseda, R., A. J. Schain, A. Melo-Carrillo, J. Tien, J. Stratton, F. Mai, A. M. Strassman, and R. Burstein. 2020. 'Fluorescently-labeled fremanezumab is distributed to sensory and autonomic ganglia and the dura but not to the brain of rats with uncompromised blood brain barrier', *Cephalalgia*, 40: 229-40.

Paige, C., I. Plasencia-Fernandez, M. Kume, M. Papalampropoulou-Tsiridou, L. E. Lorenzo, E. T. David, L. He, G. L. Mejia, C. Driskill, F. Ferrini, A. L. Feldhaus, L. F. Garcia-Martinez, A. N. Akopian, Y. De Koninck, G. Dussor, and T. J. Price. 2022. 'A Female-Specific Role for Calcitonin Gene-Related Peptide (CGRP) in Rodent Pain Models', *J Neurosci*, 42: 1930-44.

Recober, A., A. Kuburas, Z. Zhang, J. A. Wemmie, M. G. Anderson, and A. F. Russo. 2009. 'Role of calcitonin gene-related peptide in light-aversive behavior: implications for migraine', *J Neurosci*, 29: 8798-804.

Russo, A. F. 2015. 'Calcitonin gene-related peptide (CGRP): a new target for migraine', *Annu Rev Pharmacol Toxicol*, 55: 533-52.

Russo, Cinzia Valeria, Francesco Saccà, Simone Braca, Mattia Sansone, Angelo Miele, Antonio Stornaiuolo, and Roberto De Simone. 2023. 'Anti-calcitonin gene-related peptide monoclonal antibodies for the treatment of vestibular migraine: A prospective observational cohort study', *Cephalalgia*, 43: 03331024231161809.

374 Tian, R., Y. Zhang, Q. Pan, Y. Wang, Q. Wen, X. Fan, G. Qin, D. Zhang, L. Chen, Y. Zhang, and J.
375 Zhou. 2022. 'Calcitonin gene-related peptide receptor antagonist BIBN4096BS regulates
376 synaptic transmission in the vestibular nucleus and improves vestibular function via
377 PKC/ERK/CREB pathway in an experimental chronic migraine rat model', *J Headache Pain*, 23:
378 35.

379 Zhang, Y., Y. Zhang, K. Tian, Y. Wang, X. Fan, Q. Pan, G. Qin, D. Zhang, L. Chen, and J. Zhou. 2020.
380 'Calcitonin gene-related peptide facilitates sensitization of the vestibular nucleus in a rat model
381 of chronic migraine', *J Headache Pain*, 21: 72.

382

383

384

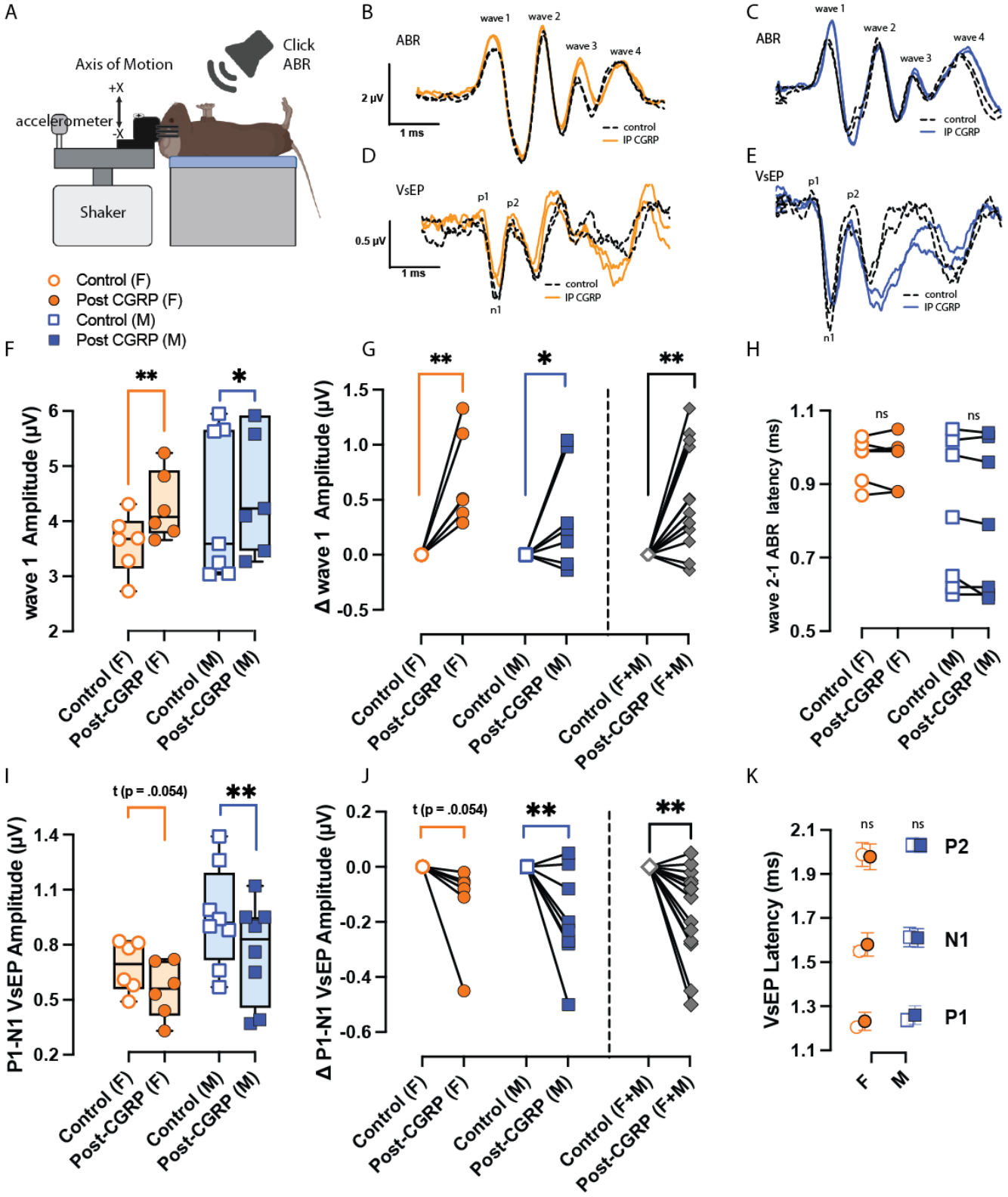
A
Axis of Motion
+X
-X
accelerometer
Shaker
Click
ABR
Control (F)
Post CGRP (F)
Control (M)
Post CGRP (M)
B
ABR
wave 1
wave 2
wave 3
wave 4
2 µV
1 ms
control
IP CGRP
C
ABR
wave 1
wave 2
wave 3
wave 4
control
IP CGRP
D
VsEP
p1
p2
n1
0.5 µV
1 ms
control
IP CGRP
E
VsEP
p1
p2
n1
control
IP CGRP
F
wave 1 Amplitude (µV)
Control (F)
Post-CGRP (F)
Control (M)
Post-CGRP (M)
G
Δ wave 1 Amplitude (µV)
Control (F)
Post-CGRP (F)
Control (M)
Post-CGRP (M)
Control (F+M)
Post-CGRP (F+M)
H
wave 2-1 ABR latency (ms)
ns
Control (F)
Post-CGRP (F)
Control (M)
Post-CGRP (M)
I
P1-N1 VsEP Amplitude (µV)
t (p = .0.054)
Control (F)
Post-CGRP (F)
Control (M)
Post-CGRP (M)
J
Δ P1-N1 VsEP Amplitude (µV)
t (p = .0.054)
Control (F)
Post-CGRP (F)
Control (M)
Post-CGRP (M)
Control (F+M)
Post-CGRP (F+M)
K
VsEP Latency (ms)
ns
P2
N1
P1
F
M

Fig. 1

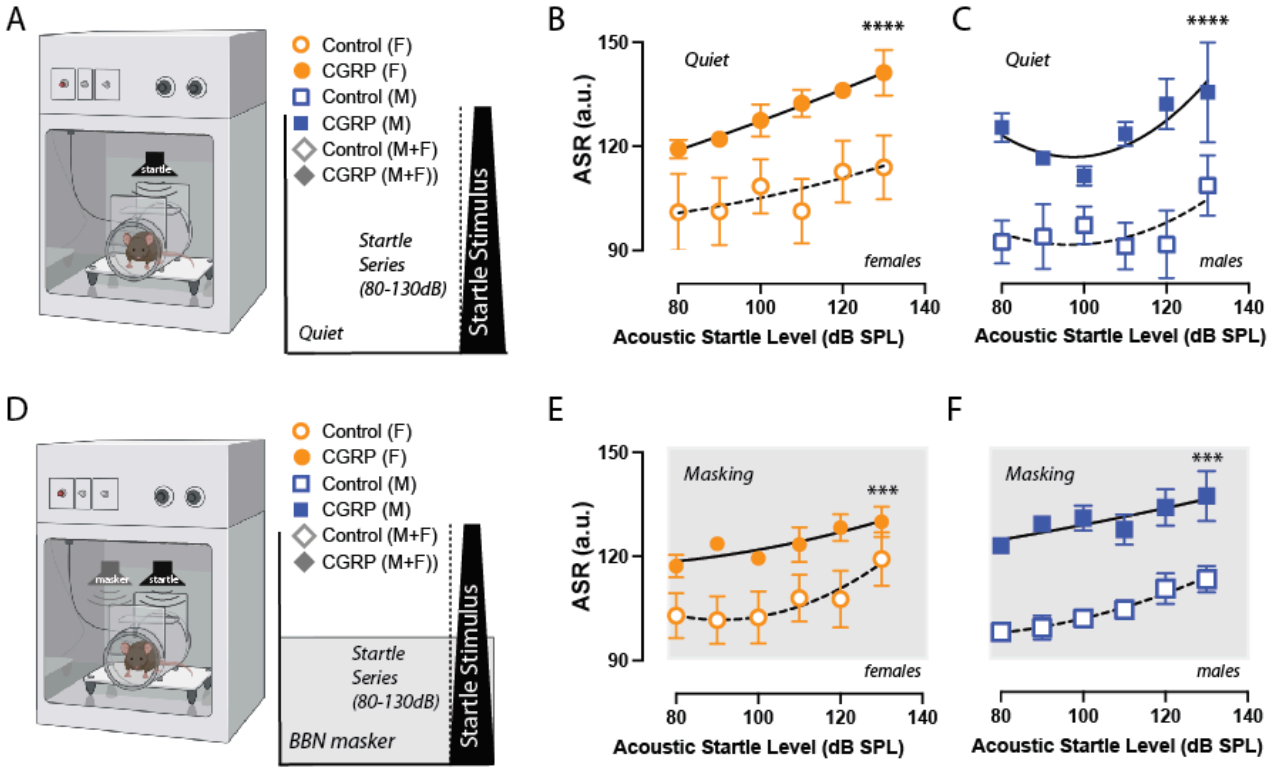
A
Control (F)
CGRP (F)
Control (M)
CGRP (M)
Control (M+F)
CGRP (M+F))
Startle Series (80-130dB)
Quiet
Startle Stimulus
B
Quiet
****
ASR (a.u.)
150
120
90
females
80
100
120
140
Acoustic Startle Level (dB SPL)
C
Quiet
****
males
Acoustic Startle Level (dB SPL)
D
Control (F)
CGRP (F)
Control (M)
CGRP (M)
Control (M+F)
CGRP (M+F))
Startle Series (80-130dB)
BBN masker
Startle Stimulus
E
Masking
***
ASR (a.u.)
150
120
90
females
Acoustic Startle Level (dB SPL)
F
Masking
***
males
Acoustic Startle Level (dB SPL)

Fig. 2

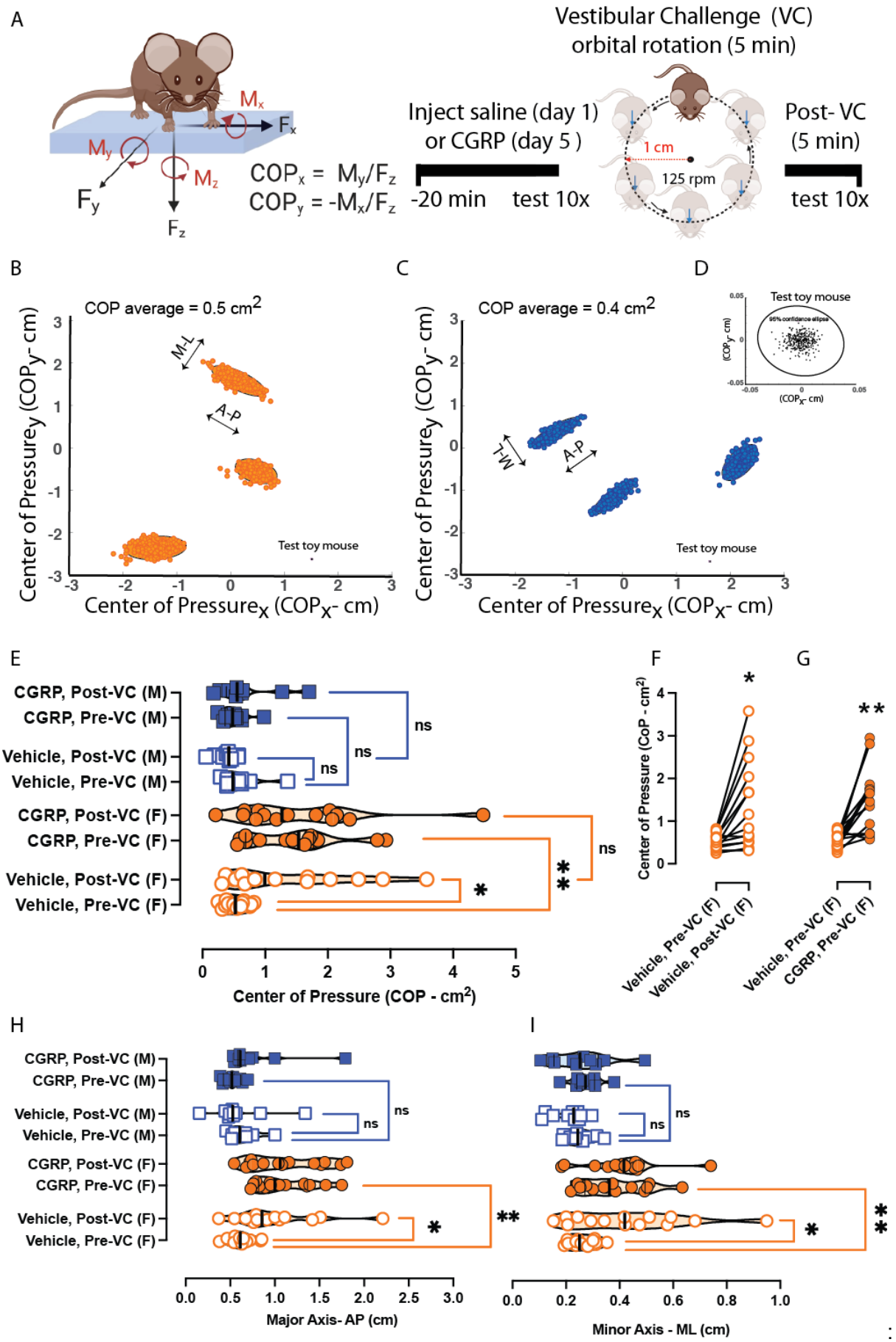
A
Vestibular Challenge (VC)
orbital rotation (5 min)
Inject saline (day 1)
or CGRP (day 5)
Post- VC
(5 min)
1 cm
125 rpm
-20 min
test 10x
test 10x
COPx = My/Fz
COPy = -Mx/Fz
B
COP average = 0.5 cm2
M-L
A-P
Test toy mouse
Center of Pressurey (COPy- cm)
Center of Pressurex (COPx- cm)
C
COP average = 0.4 cm2
M-L
A-P
Test toy mouse
Center of Pressurey (COPy- cm)
Center of Pressurex (COPx- cm)
D
Test toy mouse
E
CGRP, Post-VC (M)
CGRP, Pre-VC (M)
Vehicle, Post-VC (M)
Vehicle, Pre-VC (M)
CGRP, Post-VC (F)
CGRP, Pre-VC (F)
Vehicle, Post-VC (F)
Vehicle, Pre-VC (F)
ns
Center of Pressure (COP - cm2)
F
G
Center of Pressure (CoP - cm2)
Vehicle, Pre-VC (F)
Vehicle, Post-VC (F)
CGRP, Pre-VC (F)
H
I
Major Axis- AP (cm)
Minor Axis - ML (cm)

Fig. 3

394 **Figure Legends:**

395 **Fig. 1.** ***A,*** Schematic illustrating mouse setup for VsEP/ABR recordings captured during baseline
396 (control) and 20-30 minutes after intraperitoneal (IP) injections of either PBS vehicle or 0.1 mg/kg
397 CGRP in male (M) and female (F) C57BL6/J mice***. B-C,*** Representative click-evoked ABR waveforms -
398 in duplicate -were collected for ABR at a maximal intensity of 100 dB SPL, and waves were labeled
399 (wave1 – wave 4). ***D-E,*** Likewise, representative VsEP waveforms were collected at +6 dB re: 1 g/ms
400 having three, labeled response peaks (p1, n1, and p2). Orange and blue colors are used to distinguish
401 female and male tracings post-CGRP, respectively. The following symbols and colors are used: female
402 - orange, male - square, control - open, CGRP - closed. Sample sizes list - ABR (n = 6F/7M), VsEP (n =
403 6F/8M). ***G & J,*** Before/after plots indicate the change in amplitude post-CGRP compared to a control
404 response normalized to zero. ***F-G***, A significant increase is seen in wave 1 ABR amplitudes post CGRP
405 for female ($p = 0.005$), male ($p = 0.05$), and also when sexes are pooled ($p = 0.001$). ***I-J,*** For VsEPs, a
406 statistically significant decrease in P1-N1 VsEP amplitudes was seen in males ($p < 0.01$), a trend was
407 seen in females (t ($p = 0.054$)), and when sexes are pooled ($p = 0.002$). IP CGRP had no significant
408 effects on ***(H)*** ABR or ***(K)*** VsEP latencies. No amplitude or latency effects were observed in a separate
409 group of mice (*n* = 4) that were tested for baseline control and IP saline (not shown).

410

411 **Fig. 2. Systemic CGRP increases Acoustic Startle Responses (ASR) in both quiet and**
412 **background noise, suggesting increased sound sensitivity.** ***A,*** Schematic of startle stimulus
413 presented in otherwise quiet background conditions. ***B-C***, In female mice (***B***, n = 6), and male mice (***C***,
414 n=6), there were significant differences between vehicle and IP CGRP ASR measures in quiet
415 conditions ($p < 0.0001$). All mice were more sensitive to the same sound level of ASR stimulus after
416 being injected with CGRP. ***D,*** Schematic of startle stimulus embedded in continuous 60dB SPL
417 broadband background noise. ***E-F,*** ASR embedded in noise was also more sensitive to same sound
418 level after CGRP injection as shown for female mice (***E***, n = 6), male mice (***F***, n = 6), ($p < 0.001$). All
419 mice were more sensitive to the same level of ASR stimulus whether delivered in quiet or in BBN after
420 being injected with CGRP. Moreover, all mice showed ASR increases with sound level from 80 to
421 130dB SPL with near maximal startle is elicited by 130 dB SPL stimulus levels. Error bars are SEMs.

422

423 **Fig. 3. CGRP and VC's effects on postural sway.** Symbols and colors are depicted in a similar
424 scheme as previous figures. ***A,*** Timeline involved mice being assessed for effects of IP vehicle control
425 (saline) or IP CGRP on day 1 or day 5, respectively. A 5-minute orbital rotation (125 rpm for 5 minutes,
426 orbital radius = 1 cm) was used as the vestibular challenge, and mice were repeatedly tested (n =
427 14F/10M). ***B-C,*** Group 95% ellipse areas during pre-VC testing were computed to be 0.50 ± 0.06 cm^2
428 for females and 0.40 ± 0.04 cm^2 for males. ***D,*** A toy mouse was measured to be 0.02 ± 0.0005 cm^2 for
429 comparison with live animals. ***E,*** During IP CGRP pre-VC tests, females had higher 95% ellipse areas
430 compared to males by 0.96 ± 0.19 cm^2 ($p = 0.01$). ***F,*** Females exhibit greater sway after vestibular
431 challenge with vehicle injection ($p = 0.02$). ***G,*** Before-after plot shows during pre-VC testing in females,
432 IP CGRP caused increased 95% ellipse areas by 0.94 ± 0.23 cm^2 when compared to their IP vehicle
433 response ($p = 0.003$). ***H,*** For Pre-VC AP sway in females, IP CGRP increased AP ellipse lengths by
434 0.49 + 0.10 cm compared to IP vehicle ($p = 0.001$). An increase in female AP lengths was detected in
435 IP vehicle from pre-VC to post-VC, but this was trending ($p = 0.02$). ***I,*** For Pre-VC ML sway in females,
436 IP CGRP increased ML ellipse lengths by 0.12 + 0.03 cm compared to IP vehicle, ($p = 0.02$). In IP-
437 vehicle treated females, an increase (trend) in ML ellipse lengths is observed from pre-VC to post-VC
438 ($p = 0.02$), and IP CGRP-treated females had increased ML ellipse lengths compared to their vehicle
439 response by 0.12 + 0.03 cm ($p = 0.007$).